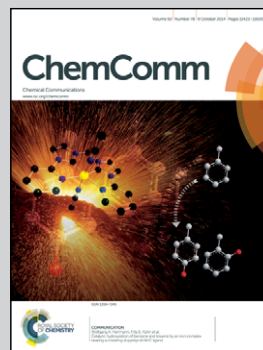**Showcasing research from the laboratories of Sanehiro Muromachi, Methane Hydrate Research Centre, National Institute of Advanced Industrial Science and Technology (AIST), Tsukuba, Japan, Ryo Ohmura, Department of Mechanical Engineering, Keio University, Yokohama, Japan, and John A. Ripmeester, National Research Council of Canada, Ottawa, Canada.**

Guest-induced symmetry lowering of an ionic clathrate material for carbon capture

CO_2 gas stabilizes a particular ionic clathrate hydrate structure that allows the most efficient incorporation of CO_2 molecules. The structure was characterized by a set of methods, including single crystal X-ray diffraction, NMR, and MD simulations.

As featured in:

ChemComm
Chemical Communications

COMMUNICATION
Muromachi, Hermann, Ohmura, Ripmeester et al.
Guest-induced hydration number and structural transition in an ionic clathrate hydrate revealed by Raman spectroscopy

See S. Muromachi *et al.*,
Chem. Commun., 2014, **50**, 11476.

ROYAL SOCIETY
OF CHEMISTRY

www.rsc.org/chemcomm

Registered charity number: 207890

COMMUNICATION

Guest-induced symmetry lowering of an ionic clathrate material for carbon capture†

S. Muromachi,*[a] K. A. Udachin,[b] K. Shin,[c] S. Alavi,[bd] I. L. Moudrakovski,[d] R. Ohmura[e] and J. A. Ripmeester[b]

We report a new lattice structure of the ionic clathrate hydrate of tetra-*n*-butylammonium bromide induced by guest CO_2 molecules, which is found to provide high CO_2 storage capacity. The structure was characterized by a set of methods, including single crystal X-ray diffraction, NMR, and MD simulations.

Gas capture by guest–host compounds is a technology which has a possibility to mitigate a specific gas from a gas mixture with low energy consumption and not accompanied by an irreversible chemical reaction.[1] Ionic clathrate hydrates are a class of guest–host materials in which large ionic guest species, primarily substituted ammonium or phosphonium salts, are incorporated into a solid ice-like hydrogen-bonded water framework.[2] They are generally formed from aqueous solutions, and have higher melting temperatures than ice, which makes these materials suitable for applications such as cool-energy storage and gas separation/storage.[3–6] The interest in ionic clathrate hydrates lies in the fact that the small dodecahedral (D) water cages formed in the lattice are available for occupancy by small gas-phase guest species, *e.g.*, CO_2, CH_4 and H_2, generally under milder conditions as compared to the pure small-guest canonical clathrate hydrates. The tetra-*n*-butylammonium bromide (TBAB) + CO_2 hydrate has been a very popular system for investigation and there have been a number of reports on the modeling of the TBAB + CO_2 hydrate.[7] However, the work reported here reinforces the need to have good structural information as the currently available models for the ionic hydrates depend on a number of unfounded assumptions.

For example, at a CO_2 gas pressure of 4 MPa, the TBAB ionic hydrate, encapsulating CO_2 guests, is formed at 291 K which is ∼10 K higher than the temperature needed to synthesize the pure CO_2 clathrate hydrate at the same pressure.[4] In the canonical clathrate hydrates, several guest-induced modifications of the host water framework have been reported.[8] Such host-framework rearrangements in the presence of a gaseous guest allow the most efficient incorporation of the guest in the resulting structure. The occupancy of CO_2 as a guest substance in hydrate cages is affected by guest–host and/or guest–guest interactions,[9,10] however, a lattice structural transition induced by CO_2 has not been reported.

Herein, we report a new CO_2-driven ionic clathrate-hydrate structure transformation which leads to efficient CO_2 encapsulation. To see how the guest gas molecules stabilize/destabilize the ionic clathrate hydrate, we performed single crystal X-ray diffraction (SCXRD) measurements at 100 K on the TBAB + CO_2 ionic clathrate hydrate. The crystals were synthesized from an aqueous TBAB solution with mole fraction x_{TBAB} = 0.0064 under CO_2 pressure P = 1.08 MPa at temperature T = 282.65 K. The experimental details and a figure of the crystal structure are given in the ESI.† The crystallographic information is summarized in the footnote.‡ The TBA cation is encapsulated in super cages derived from four of the large canonical clathrate cages, and Br^- replaces water molecules in the lattice.[2] Unexpectedly, in the presence of CO_2, only the orthorhombic *Imma* crystal structure was found, whereas the TBAB hydrate formed without a guest gas has the tetragonal (TBAB·26H$_2$O) and orthorhombic (TBAB·38H$_2$O) phases as the most stable phases, with yet other phases also observed. The determined space group *Imma* has the same point group but a different lattice from *Pmma* observed for TBAB· 38H$_2$O.[11] The symmetry of the *Imma* structure is lower because of the doubling of the unit cell size in the direction of the *b*-axis compared to the pure *Pmma* hydrate. This lattice change evidently arises from the asymmetrical distributions of the incorporated CO_2 molecules in the dodecahedral (D) cages of the *Imma* hydrate and is not related to structural changes in the TBAB and water framework upon CO_2 encapsulation. The CO_2 molecules occupy the two symmetry-distinct dodecahedral-cages as shown in Fig. 1

[a] *Methane Hydrate Research Centre, National Institute of Advanced Industrial Science and Technology (AIST), 16-1 Onogawa, Tsukuba, 305-8569 Japan. E-mail: s-muromachi@aist.go.jp*
[b] *National Research Council of Canada, Canada*
[c] *Korea Advanced Institute of Science and Technology (KAIST), Korea*
[d] *University of Ottawa, Canada*
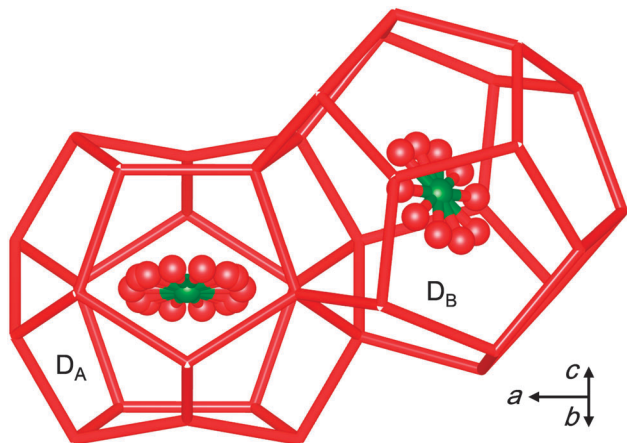[e] *Keio University, Japan*

Fig. 1 The highly distorted D_A and regular shaped D_B dodecahedral cages in the TBAB + CO_2 structure. The arrow denotes the direction of the unit cell axes.

Fig. 2 (A) Experimental ^{13}C CP MAS spectrum of the $^{13}CO_2 \cdot TBAB \cdot 38H_2O$ hydrate obtained under a field of 9.4 T (Larmor frequency of 100.67 MHz) at 173 K and a spinning speed of 2975 Hz. (B) Simulation of the experimental spectrum with a model accounting for the spectral intensity spread in the spinning sidebands.

(and Fig. S1 of the ESI†), and include the highly distorted cages D_A and more regular dodecahedral cages D_B. The chemical formula of the empty host framework can be written as TBAB·38H₂O·D_A·2D_B.

In the crystal structure, the fraction of D_A cages occupied by CO_2 is almost twice that of the D_B cages, *i.e.*, 0.867 and 0.490, respectively. As shown in Fig. 1, the water molecules forming the D_A cage are displaced by the *n*-butyl chains of the [TBA]⁺ ion and pushed inward by the Br⁻ ions. As a result, the lattice is highly distorted along a direction perpendicular to the plane of the confined CO_2 molecules. This clearly differs from the structure of D cages holding CO_2 in canonical clathrate hydrate phases. The D_A and D_B cages have similar volumes, *i.e.*, 153 and 160 Å³, respectively. As reported in Table S2 of the ESI,† three crystal samples of the TBAB + CO_2 hydrate formed under the different *P-T-x* conditions had the same orthorhombic *Imma* structure. The preference of an orthorhombic hydrate structure over the tetragonal structure in the presence of CO_2 (or small-guest) can be rationalized by considering the unit cell volume per 5^{12} cages, *i.e.*, 76H₂O/6 D cages for the orthorhombic phase and 164H₂O/10 D cages for the tetragonal TBAB phase.[2,6] Thus application of Le Chatelier's principle suggests that the orthorhombic structure gives the largest pressure drop and the greatest stabilization effect as a result of CO_2 incorporation into the D cages.

To study the CO_2 guest environments and occupancies in the D_A and D_B cages, CP-MAS ^{13}C NMR spectra of the TBAB + CO_2 solid phase were obtained, as shown in Fig. 2. This sample was made by exposing the solid TBAB hydrate to CO_2 gas under pressure; see the ESI† for details of the sample preparation. The spectra demonstrate a complex overlap of the isotropic signals and spinning sidebands near 125 ppm of CO_2 guests in three distinct sites and TBAB in the lattice of the ionic clathrate. The ratio of the integrated intensities for the hydrate cage signals with isotropic chemical shifts at 124.87 and 125.13 ppm is less than unity, *i.e.*, 0.54 (30/55), which is consistent with the relationship between the total number of CO_2 guests in the D_A and D_B cages determined by the SCXRD, $N(D_A)/N(D_B)$ = 0.867/(2 × 0.490) = 0.88. Both the signal intensities in the NMR
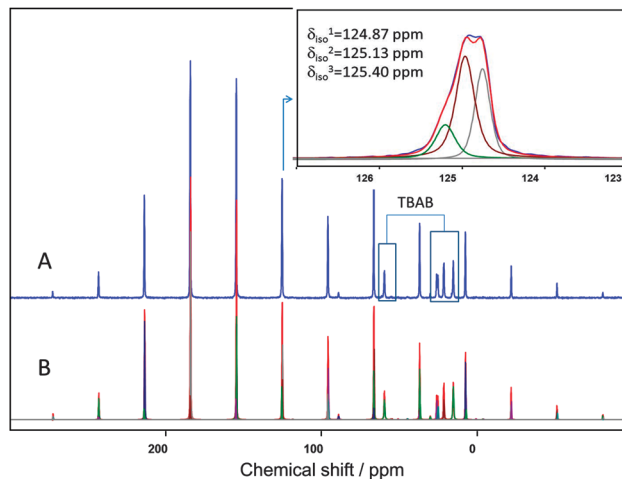
spectrum and the CO_2 occupancies in the SCXRD structure indicate a smaller CO_2 population in the more abundant D_B cages.

The isotropic chemical shifts for CO_2 residing in D cages in this work are close to the ∼128 ppm chemical shifts of CO_2 guests previously reported in other clathrate hydrate phases.[7] The difference in chemical shifts from 128 ppm in D cages reported for other hydrates to ∼125 ppm in the presently found D_A and D_B cages can be related to the smaller sizes of the latter cages, or to the presence of the charged Br⁻ and [TBA]⁺ groups in close proximity, and also to the fact that previous chemical shift data were reported for stationary samples thus offering lower accuracy because of the broad powder patterns. The assignment of the low intensity signal at 125.40 ppm is less certain, and could arise from a different ionic clathrate phase formed under the non-equilibrium sample preparation conditions of the powder NMR sample. This is verified by powder X-ray diffraction (PXRD) measurements of the TBAB + CO_2 phases formed under conditions similar to the preparation of the NMR samples. The PXRD patterns given in the ESI† show that the sample contained both orthorhombic and tetragonal phases, and thus the two main signals for CO_2 (natural abundance) appearing at 124.85 and 125.06 ppm of the ^{13}C NMR spectrum shown in Fig. S5 (ESI†) should originate from the orthorhombic phase and the additional small peak at 125.30 ppm from a small fraction of the tetragonal phase, respectively.

Guest dynamics were also studied using the MD simulation methodology with details outlined in the ESI.† The CO_2 guests were found to have restricted, but different spatial distributions/motions in D_A and D_B cages. The sampled orientations of the CO_2 guest molecules in the D_A and D_B cages with respect to the lattice *b*-direction (corresponding to the flattened direction of the D_A cage) are reported in the ESI.†

The dynamics of the CO_2 guest motion were also studied using the orientation autocorrelation function (OACF) around the molecular axis. If $\phi(t)$ is the rotation angle of the unit vector
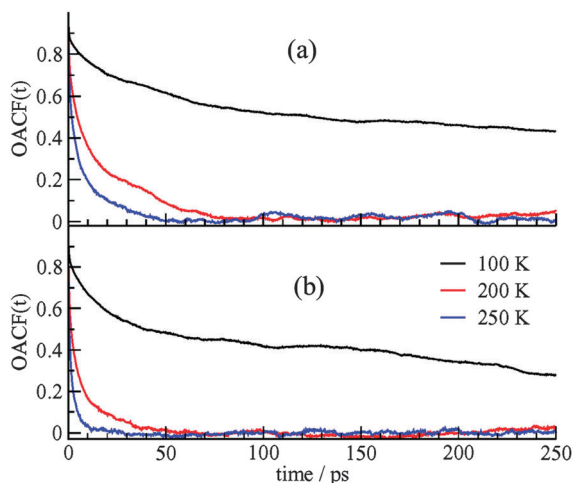
Fig. 3 The OACF for CO_2 molecules in (a) the D_A cages, (b) the D_B cages. The size of the D_A cages is smaller and the orientation correlations decay more slowly for molecules in these cages.

along the direction of the CO_2 molecular axis at time t, $\mu(t)$, with respect to the vector orientation at time 0, $\mu(0)$, the OACF defined as the ensemble average of the first moment of the Legendre polynomial for the rotation angle, $\langle P_1(t)\rangle$, is presented as,

$$\langle P_1(t)\rangle = \langle \mu(t)\cdot\mu(0)\rangle = \langle \cos\theta(t)\rangle \qquad (1)$$

where the brackets $\langle\rangle$ indicate and ensemble the average over all CO_2 molecules in the separate D_A or D_B cages. The behaviors of $\langle P_1(t)\rangle$ for CO_2 guests in the two cages are given in Fig. 3. The D_A cages are smaller and the orientation correlations for CO_2 guests in these cages decay more slowly at all temperatures.

The simulations show that the lattice vibrations of tetra-n-butylammonium and bromide groups about their equilibrium positions are small and they are kept in place by electrostatic and van der Waals interactions with the neighboring water molecules. This is particularly interesting with regard to the Br^- lattice vibrations as this ion may seem to be relatively free to move in the ionic hydrate lattice. The lattice site of injection of the Br^- anion can be the site of Bjerrum L-defects[12] in the neighboring water molecule lattice. In the simulation, water molecules show relatively slow rotational dynamics in the lattice. This is consistent with experiments since the ^{13}C NMR powder patterns are broad and look distributed at around 200 K, much the same as for the large cage in the sI hydrate at this temperature. The water dynamics in the double hydrate of tetrahydrofuran + CO_2 are much faster at temperatures around 200 K.[10]

The presence of CO_2 guests lowered the symmetry of the original TBAB hydrate structure formed without small guest molecules. The CO_2 gas storage capacities in the two types of D cages in the structure differ significantly because of the size and shape differences of the cages. This demonstrates that the shape of the guest molecules is a secondary factor for determining the gas storage capacity of the ionic clathrates in addition to the primary factor of molecular size. From a practical

point of view, our experiments show that upon exposure to relatively mild CO_2 pressures and controlled temperature/composition conditions, it is possible to selectively drive the formation of the ionic clathrate hydrate towards the orthorhombic TBAB·38H_2O·nCO_2 phase which is the most effective one for carbon capture. We note that the large difference in gas-holding capacity of the D_A and D_B small cage types in the hydrate is of key importance in developing satisfactory models that will account for a variety.

Notes and references

‡ $C_{17.85}H_{111}BrNO_{41.69}$, M_r = 1087.28, crystal dimensions: 0.6 × 0.4 × 0.2, orthorhombic *Imma*, a = 21.0197(7), b = 25.2728(8), c = 12.0096(4) Å, V = 6379.8(4) Å^3, Z = 4, T = 100.0(1) K, ρ_{calcd} = 1.132 g cm^{-3}, μ = 0.730, radiation and wavelength: Mo Kα and 0.71070 Å, $2\theta_{max}$ = 72.76, no. of measured and independent reflections: 87 521 and 8002, R_{int} = 0.0363, final $R(I > 2\sigma(I))$ indices: R_1 = 0.0266, wR_2 = 0.0589. The structure was solved by direct methods using the SHELXTL suite of programs[13] and visualized by VESTA.[14] CCDC 963037.

1 *Comprehensive Supramolecular Chemistry*, Supramolecular Technology, ed. D. N. Reinhoudt, Pergamon, Oxford, 1996, vol. 10; D. M. D'Alessandro, B. Smit and J. R. Long, *Angew. Chem., Int. Ed.*, 2010, **49**, 6038; S. D. Kenarsari, D. Yang, G. Jiang, S. Zhang, J. Wang, A. G. Russell, Q. Wei and M. Fan, *RSC Adv.*, 2013, **3**, 22739.
2 M. Bonamico, G. A. Jeffrey and R. K. McMullan, *J. Chem. Phys.*, 1962, **37**, 2219; R. K. McMullan, G. A. Jeffrey and M. Bonamico, *J. Chem. Phys.*, 1963, **39**, 3295; D. W. Davidson, in *Water. A Comprehensive Treatise*, ed. F. Franks, Plenum Press, New York, NY, 1973; G. A. Jeffrey, in *Inclusion Compd.*, ed. J. L. Atwood, J. E. D. Davies and D. D. MacNicol, Academic Press, London, 1984, ch. 5, vol. 1.
3 A. Chapoy, R. Anderson and B. Tohidi, *J. Am. Chem. Soc.*, 2007, **129**, 746; N. H. Duc, F. Chauvy and J.-M. Herri, *Energy Convers. Manage.*, 2007, **48**, 1313; D. Zhong and P. Englezos, *Energy Fuels*, 2012, **26**, 2098.
4 N. Ye and P. Zhang, *J. Chem. Eng. Data*, 2012, **57**, 1557.
5 H. Oyama, W. Shimada, T. Ebinuma, Y. Kamata, S. Takeya, T. Uchida, J. Nagao and H. Narita, *Fluid Phase Equilib.*, 2005, **234**, 131; K. Sato, H. Tokutomi and R. Ohmura, *Fluid Phase Equilib.*, 2013, **337**, 115.
6 S. Muromachi, S. Takeya, Y. Yamamoto and R. Ohmura, *CrystEngComm*, 2014, **16**, 2056.
7 X. Liao, X. Guo, Y. Zhao, Y. Wang, Q. Sun, A. Liu, C. Sun and G. Chen, *Ind. Eng. Chem. Res.*, 2013, **52**, 18440; W. Lin, D. Dalmazzone, W. Fürst, A. Delahaye, L. Fournaison and P. Clain, *J. Chem. Eng. Data*, 2013, **58**, 2233; A. Joshi, P. Mekala and J. S. Sangwai, *J. Nat. Gas Chem.*, 2012, **21**, 459; P. Paricaud, *J. Phys. Chem. B*, 2011, **115**, 288; M. Kwaterski and J.-M. Herri, *Fluid Phase Equilib.*, 2014, **371**, 22; P. Babu, W. I. Chin, R. Kumar and P. Linga, *Ind. Eng. Chem. Res.*, 2014, **53**, 4878.
8 K. Shin, S. Choi, J.-H. Cha and H. Lee, *J. Am. Chem. Soc.*, 2008, **130**, 7180; K. A. Udachin, C. I. Ratcliffe, G. D. Enright and J. A. Ripmeester, *Angew. Chem., Int. Ed.*, 2008, **47**, 9704; K. Shin, Y. Kim, T. A. Strobel, P. S. R. Prasad, T. Sugahara, H. Lee, E. D. Sloan, A. K. Sum and C. A. Koh, *J. Phys. Chem. A*, 2009, **113**, 6415; K. Shin, K. A. Udachin, I. L. Moudrakovski, D. M. Leek, S. Alavi, C. I. Ratcliffe and J. A. Ripmeester, *Proc. Natl. Acad. Sci. U. S. A.*, 2013, **110**, 8441; K. Shin, R. Kumar, K. A. Udachin, S. Alavi and J. A. Ripmeester, *Proc. Natl. Acad. Sci. U. S. A.*, 2012, **109**, 14785; K. Shin, I. L. Moudrakovski,

M. D. Davari, S. Alavi, C. I. Ratcliffe and J. A. Ripmeester, *CrystEng-Comm*, 2014, DOI: 10.1039/c3ce41661e.

9 J. A. Ripmeester and C. I. Ratcliffe, *Energy Fuels*, 1998, **12**, 197; K. A. Udachin, C. I. Ratcliffe and J. A. Ripmeester, *J. Phys. Chem. B*, 2001, **105**, 4200; S. Alavi, P. Dornan and T. K. Woo, *ChemPhysChem*, 2008, **9**, 911.

10 S. Alavi and J. A. Ripmeester, *J. Chem. Phys.*, 2012, **137**, 054712; K. Tezuka, R. Shen, T. Watanabe, S. Takeya, S. Alavi, J. A. Ripmeester and R. Ohmura, *Chem. Commun.*, 2013, **49**, 505.

11 L. A. Gaponenko, S. F. Solodovnikov, Y. A. Dyadin, L. S. Aladko and T. M. Polyanskaya, *Zh. Strukt. Khim.*, 1984, **25**, 175; W. Shimada, M. Shiro, H. Kondo, S. Takeya, H. Oyama, T. Ebinuma and H. Narita, *Acta Crystallogr., Sect. C*, 2005, **61**, o65.

12 N. Bjerrum, *Science*, 1952, **115**, 385.

13 G. M. Sheldrick, *Acta Crystallogr., Sect. A*, 1990, **46**, 467; G. M. Sheldrick, *Acta Crystallogr., Sect. A*, 1993, **49**(suppl), C53.

14 K. Momma and F. Izumi, *J. Appl. Crystallogr.*, 2011, **44**, 1272.